Progress In Electromagnetics Research C, Vol. 132, 103–115, 2023

A Meandered Inductive Loop Based RFID Tag Antenna for Luggage Tracking

Amit K. Singh* and Amit K. Singh

Abstract—In this paper, a planar tag antenna for UHF band RFID composed of a spiral ending meandered line with meandered inductive loop is presented. The presented novel compact spiral ended meandered tag having double sided meandered inductive loop microstrip dipoles scales down the extent of tag antenna and provides an upgraded conjugate impedance matching between tag antenna and semiconductor ASIC. This tag antenna operates at 866 MHz. Here, a compact UHF tag having volume of $60 \times 16 \times 1.6\,\text{mm}^3$ ($0.173\lambda \times 0.046\lambda \times 0.0046\lambda$) is testified. This antenna produces impressive reflection coefficient and is able to access detection territory of 12.6 m. The proposed RFID antenna layout is simulated in favor of reader having 4 W EIRP.

1. INTRODUCTION

In 1999, United States' Uniform Code Council (UCC) and European Article Numbering (EAN) Association, presently both known as GS1, launched an Auto-ID center in Ultra High Frequency band for developing Electronic Product Code (EPC) [1]. In Ultra-High Frequency (UHF) radio frequency identification technology, tag receives power from incoming electromagnetic waves evolving from the reader and back-scatters the signal on the way to reader. The evolution in semiconductor market in 1990s expedited the Radio Frequency Identification (RFID)-commercialization in transportation, logistics, supply chain supervision, and product tracing. In recent past years, RFID has been victorious in superseding other automatic identification techniques like barcodes, smart cards, and magnetic stripe cards, because of its advantage of providing non-line of sight connection with considerable storage. At present, RFID methodology has been accomplishing its peak in area of Hospitals, Electronic Payment Systems, Libraries, Access control, Agriculture, Marathons and many more applications [2].

In 2002, Federal Communications Commission (FCC) accredited Ultra Wide Band Radio Frequency Identification for wholesale applications and sanctioned various frequency bands for RFID applications. They are classified as Low Frequency (LF) band tags (125 to 134) kHz, High Frequency (HF) tags (13.56 MHz), UHF band tags (433 MHz, 840 to 960 MHz), and microwave frequency band tags (2.45 and 5.8 GHz). The ultra-high frequency band, i.e., 860 to 960 MHz, RFID devices have been more preferred correlated to LF and HF entities because they are able to operate for more miniaturized antennas and empower simultaneous exposure of collective tags [3]. Limited frequency band has been designated to a certain country or territory. Table 1 shows a few territory-wise granted frequency bands with regulated reader Equivalent Isotropic Radiated Power (EIRP).

The eminent UHF RFID tags exhibit better read territory but need lower transmission power. The semiconductor-chip used in UHF tag is a data storing device and capacitive in nature. For complex impedance matching with semiconductor-chip, an inductive tag antenna is used. In [4], Yao et al. present a multi-polarized RFID antenna and show how meandering microstrip open-ended lines can be used for near-field applications. The inductance as well as resonating frequency of a meander line dipole

Received 8 February 2023, Accepted 12 April 2023, Scheduled 18 April 2023
* Corresponding author: Amit Kumar Singh (amit.kumarsingh.rs.ece18@iitbhu.ac.in).
The authors are with the Electronics Engineering Department, Indian Institute of Technology (BHU), Varanasi, India.

Table 1. Territory-wise UHF band allocation.

Country/Continent	Frequency(MHz)	Power
America	902–928	4 W EIRP
China	920.5–924.5	2 W ERP
Brunei	866–869	0.5 W ERP
	923–925	2 W ERP
Europe	865–868	0.1 W ERP
	865.6–868	0.5 W ERP
	865.6–867.6	2 W ERP
	915–921	4 W ERP
India	865–867	4 W ERP
Japan	916.7–920.9	4 W EIRP
	916.7–923.5	0.5 W EIRP
Jordan	865–868	2 W ERP
Morocco	865.6–865.8	2 W ERP
	867.6–868	500 mW ERP
Oman	865.6–867.6	2 W ERP
Singapore	866–869	0.5 W ERP
	920–925	2 W ERP
Thailand	920–925	4 W EIRP
Vietnam	866–868	0.5 W ERP
	918–923	0.5 W ERP
	920–923	2 W ERP
South Africa	865.6–867.6	2 W ERP
	915.4–921	4 W EIRP

antenna is adjusted by tuning the height of the meander line, its length, and number of meanders [5]. The equivalent circuit analysis of inductively coupled loop based RFID tag for on-body application is explained in [6]. Among all these designed antennas, it is found that meander line antenna befits UHF RFID applications because of its good inductive reactance, planar geometry, and miniaturized size.

This paper presents a comprehensive analysis of a meander line RFID tag with spiral-ending coupled with two-sided Meandered Inductive Loop (MIL). Inductive-coupled loop is used for impedance matching while meandering technique is used for contraction of antenna dimensions. Hence, this hybridization produces the novelty of proposed RFID tag antenna with tiny size and better reading territory. Here, it works at 866 MHz which lies in the UHF band of India for RFID applications. It is comprehended from this paper that this antenna has adequate reading territory and compactness with respect to size contrary to erstwhile designs. Here, tag input impedance matching with semiconductor-chip Alien (Higgs-4) SOT, equivalent circuit prototype of tag, reflection coefficient, and reading territory are presented. This proposed tag was designed and simulated with High Frequency Structure Simulator of Ansys-2020R1 software.

2. PROPOSED UHF TAG

The graphics of the proposed antenna is displayed in Figure 1. The tag has the trace of 60 mm × 16 mm × 1.6 mm built on an FR4 glass epoxy substrate ($\epsilon_r = 4.4$, $\tan\delta = 0.02$) having a thickness of 1.6 mm. This antenna is designed with meandering technique for size contraction. The tag antenna consists of a symmetric double sided Meandered Inductive Loop (MIL) microstrip dipole providing remarkable

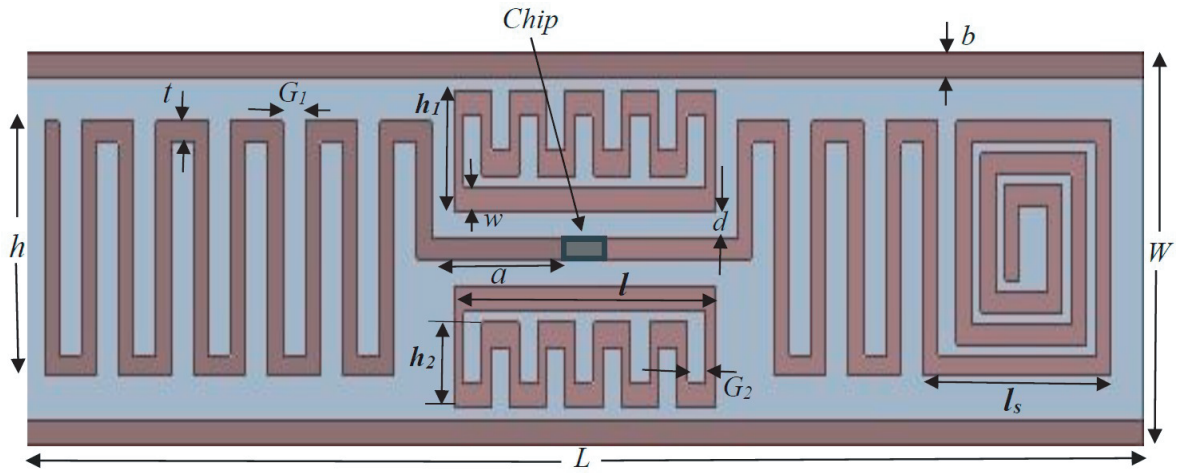

Figure 1. Schematic of the proposed antenna.

impedance matching with semiconductor-chip.

The resonating frequency is changed by alternating the spiral length, meander line height, gap, feed line, and MIL separation, and thus, tag-chip impedance matching is validated on the desired frequency. The optimum values obtained for impedance matching are shown in Table 2.

Table 2. Numerical values of optimized parameters of tag antenna.

Parameter	Value in mm	Parameter	Value in mm
L	60	W	16
a	7.2	l_s	10.1
w	1	b	1
h_1	5	G_2	1
G_1	1.2	d	0.8
t	0.8	l	14
h	10.4	h_2	3.5

The semiconductor-chip used in this article is Alien (Higgs-4) tag chip, which has the reading sensitivity of -18.5 dBm. The internal RC circuit schematic of the microchip Alien Higgs used in this article is shown in Figure 2. The semiconductor chip has the complex impedance of $20.53 - j190.95\Omega$ at 866 MHz. The internal impedance of semiconductor-chip is obtained by formula:

$$Z_{chip} = \frac{R}{1 + 4\pi^2 f^2 R^2 C^2} - j\frac{2\pi f R^2 C}{1 + 4\pi^2 f^2 R^2 C^2} \tag{1}$$

It is mandatory in scheming RFID tag that tag antenna impedance should be complex conjugated to that of semiconductor-chip for maximum power transfer. This matching is done through the binary states namely matched state and shorted state. Whenever tag antenna is matched with semiconductor-chip, the signal sent from reader is engrossed by the transducer, and consequently semiconductor-chip changes to shorting state. In this state, the tag antenna retransmits interrogator signal to reader. The input impedance matching of the tag antenna with semiconductor-chip is displayed in Figure 7(d). The obtained impedance of the tag at 866 MHz is $20.62 + j190.94\Omega$. The reflection coefficient is reckoned by the following formula in Eq. (2):

$$\Gamma_{tag} = \frac{Z_{chip} - Z_T^*}{Z_{chip} + Z_T} \tag{2}$$

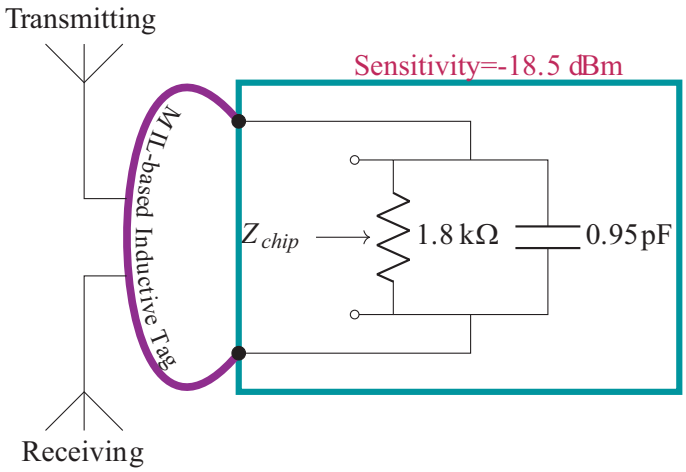

Figure 2. ALLIEN Higgs-4 IC application diagram.

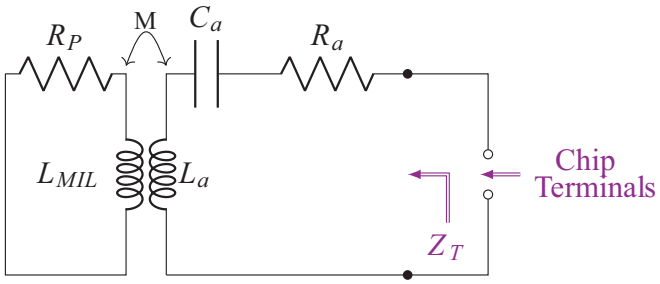

Figure 3. Spiral-ending meandered line with Meandered Inductive Coupled loop equivalent circuit.

where Z_{chip} and Z_T are semiconductor-chip and tag input impedance, respectively, where $Z_T = R_T + jX_T$ and $Z_{chip} = R_C - jX_C$.

The tag antenna comprises a two-sided MIL, which is inductively coupled with a spiral ending meandered line. After combining the spiral-ending meandered line and meandered-inductively loop, both terminals are attached to the semiconductor-chip. The equivalent circuit of this meandered-inductively coupled loop antenna is displayed in Figure 3. Tag impedance of the presented MIL based antenna is given by [7],

$$Z_T = R_T + jX_T = Z_{MIL} + \frac{(2\pi f M)^2}{Z_a} \tag{3}$$

where Z_a and Z_{MIL} are impedances of spiral-ending meandered line and MIL, respectively. M represents the mutual inductance between the inductances. Z_a is calculated by:

$$Z_a = R_{a,0} + jR_{a,0}Q_a\left(\frac{f}{f_0} - \frac{f_0}{f}\right) \tag{4a}$$

where Q_a is the quality factor, and f_0 is the resonating frequency.

$$Z_{MIL} = R_P + j2\pi f L_{MIL} \tag{4b}$$

By putting values of Z_a and Z_{MIL} from (4a) and (4b) in (3):

$$R_T = R_P + \frac{(2\pi f M)^2}{R_{a,0}\left(1 + \left[Q_a\left(\frac{f}{f_0} - \frac{f_0}{f}\right)\right]^2\right)} \tag{5a}$$

$$X_T = 2\pi f L_{MIL} - \frac{(2\pi f M)^2 Q_a \left(\frac{f}{f_0} - \frac{f_0}{f}\right)}{R_{a,0}\left(1 + \left[Q_a\left(\frac{f}{f_0} - \frac{f_0}{f}\right)\right]^2\right)} \tag{5b}$$

At the resonating frequency of tag antenna, the resistance and reactance values of input impedance of inductively coupled tag can be given by:

$$R_{T,0} = R_T\left(f = f_0\right) = R_P + \frac{(2\pi f_0 M)^2}{R_{a,0}} \tag{6a}$$

$$X_{T,0} = X_T\left(f = f_0\right) = 2\pi f_0 L_{MIL} \tag{6b}$$

Now, values of $R_{a,0}$, Q_a, and M can be calculated by given formula:

$$R_{a,0} = \eta\pi\left(\frac{P}{\lambda_0}\right)^2\left\{\frac{\lambda_0}{P}\sum_{m=0}^{\infty} J_{2m+3}\left(\frac{2P}{\lambda_0}\right)\right\} \tag{7a}$$

where P is the perimeter of loop antenna, λ_0 the wavelength at resonance frequency, and summation part represents a series of Bessel functions.

$$Q_a = \frac{2\pi f_0 L_a}{R_a} \tag{7b}$$

$$M = \frac{\mu_0 l}{2\pi}\ln\frac{h_1 + d}{d} \tag{7c}$$

The inductance of the meander-line is obtained by [8]:

$$L_m = 0.2l\left[0.022\left(\frac{w+t}{l}\right) + \ln\left(\frac{l}{w+t}\right) + 1.19\right] \text{ nH/mm} \tag{8a}$$

where l is the absolute meander-line length in mm, t the thickness in mm, and w the width in mm. The self inductance of a straight filament of any rectangular section is given by [9]:

$$L_f = \frac{\mu_0}{2\pi} l\left\{\ln\left(\frac{2l}{w+w'}\right) + 0.50049 + \left(\frac{w+w'}{3l}\right)\right\}/10^3 \text{ nH} \tag{8b}$$

where l is the length of filament, w the breadth, and w' the thickness in mm. The meandered inductively-coupled loop inductance is calculated by parallel combination of both aforementioned inductances, i.e.,

$$L_{MIL} = L_m || L_f \tag{9}$$

By using above formulas, tag antenna impedance is calculated.

The analogous RLC circuit model of proposed antenna is shown in Figure 4. The antenna structure can be split into four parts in series, i.e., spiral element, meandered antenna, MIL, and tag semiconductor

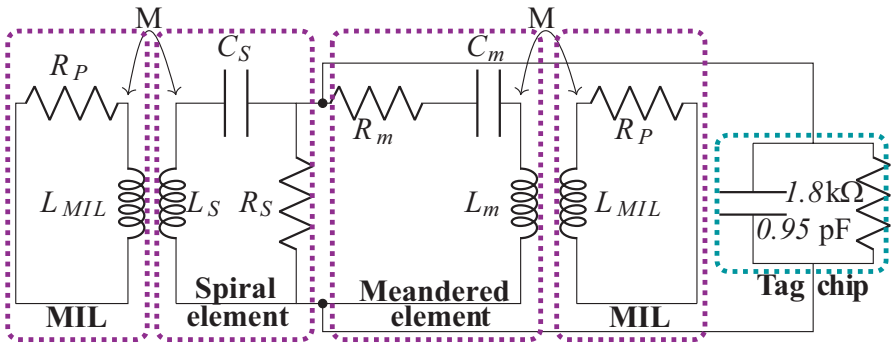

Figure 4. Equivalent circuit prototype of the proposed tag structure.

microchip. The spiral network introduces capacitance in series with meandered line capacitance; hence, capacitive reactance decreases, and inductive part of the tag impedance increases. Thus, the conjugate impedance matching is attained with the semiconductor-chip.

The tag impedance is obtained at each frequency of UHF band, and the reflection coefficient is calculated from Eq. (2) in that frequency range. The reflection coefficient for this tendered tag is displayed in Figure 5.

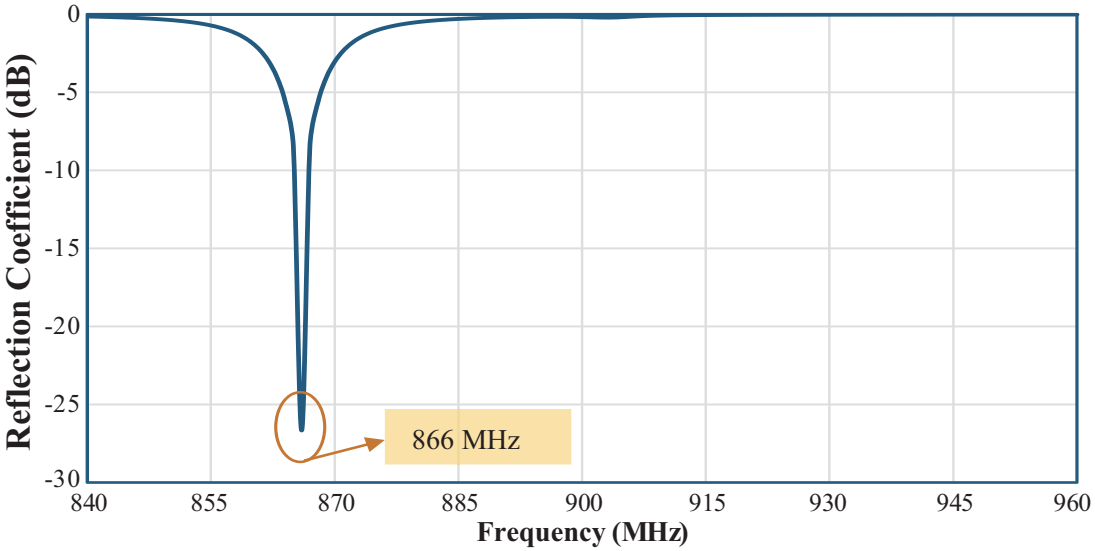

Figure 5. Reflection Coefficient of the UHF RFID tag antenna.

3. EVOLUTION STEPS

The evolution steps to achieve final tag design are shown in Figure 6. Antenna I shows the meander-line tag; Antenna II shows the spiral ending tag; Antenna III represents the hybridization of previous two which is spiral-ending meandered line tag. Antenna IV represents both sides spiral-ending with MIL tag; Antenna V is obtained by introducing MIL in Antenna III; Antenna VI represents the final

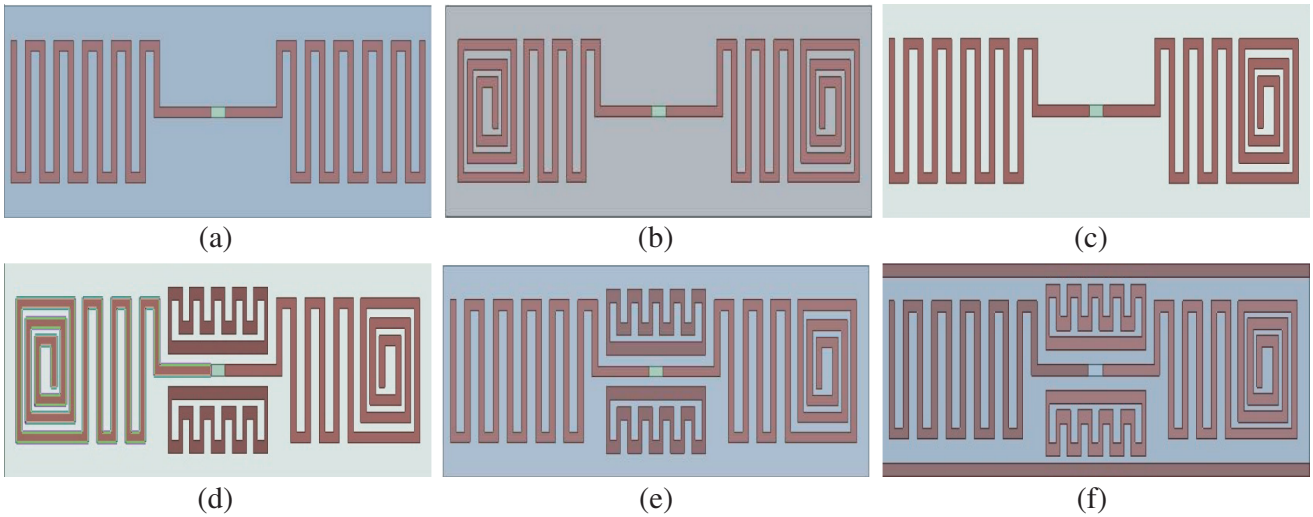

Figure 6. Evolution steps of this presented tag. (a) Antenna I. (b) Antenna II. (c) Antenna III. (d) Antenna IV. (e) Antenna V. (f) Antenna VI.

structure of designed RFID tag which is achieved by the metallization of the previous tag on top as shown in Figure 6(f).

The impedance matching graph of every step is shown in Figure 7.

From Figure 7(a), it can be seen that for Antenna I, the reactance of tag matches with semiconductor at 1331 MHz while resistance matching is achieved at 1040 MHz. This tag is not inductive in nature in the UHF band of RFID. For the impedance matching of tag to Application Specific Integrated

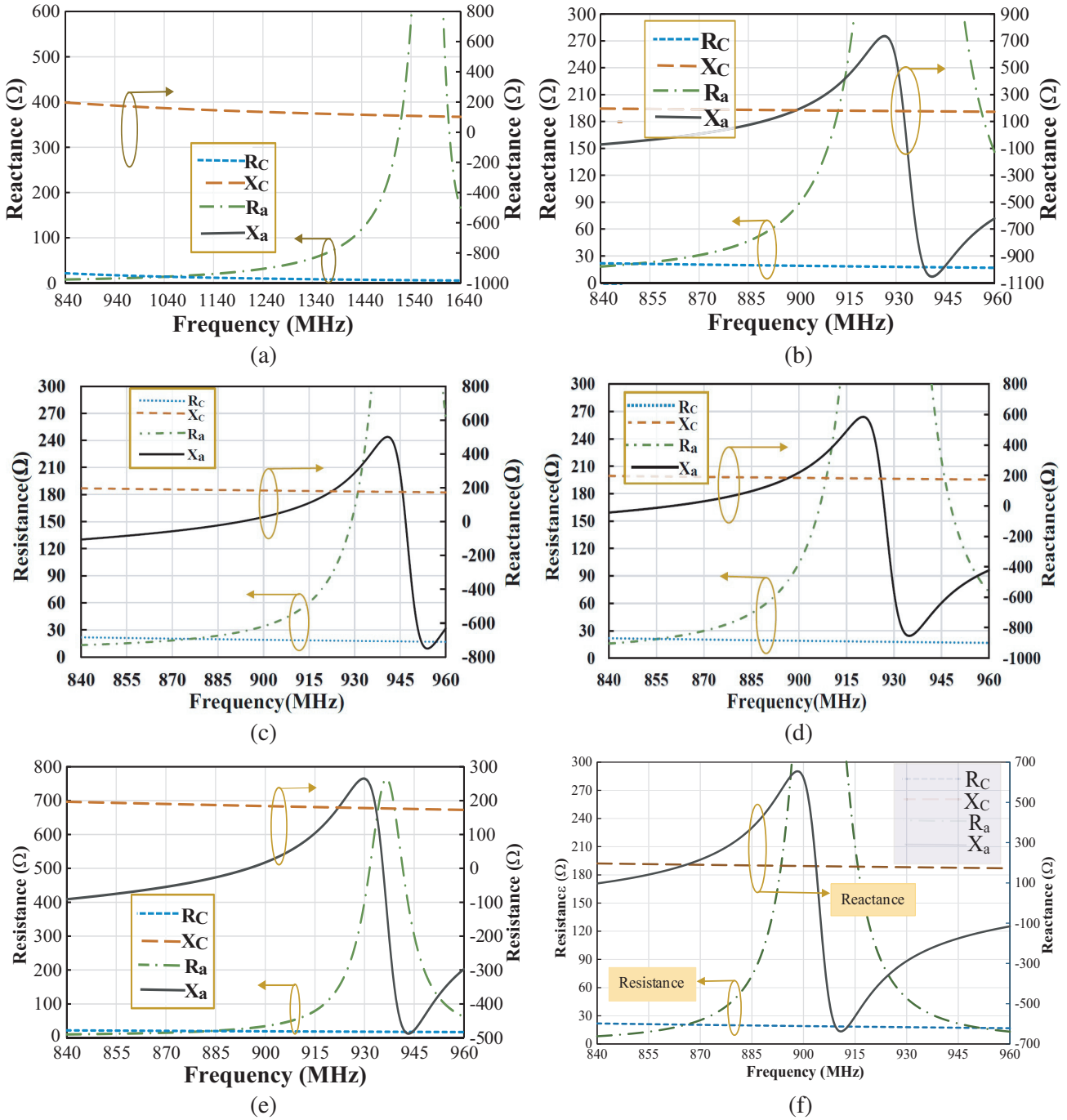

Figure 7. Input Impedances of every steps; (a) Antenna I-Complex Impedance, (b) Antenna II-Complex Impedance, (c) Antenna III-Complex Impedance, (d) Antenna IV-Complex Impedance, (e) Antenna V-Complex Impedance, (f) Antenna VI-Complex Impedance.

Circuit (ASIC), tag needs to be inductive in the operating band of frequency. After putting spirals at the end of the tag, resistance and reactance both increase for the lower frequencies, and thus tag becomes inductive in the range of 868 MHz to 933 MHz. For Antenna II, reactance matching happens at 899 MHz while that of resistance happens at 849 MHz. Thus there is 50 MHz of frequency gap. This gap is reduced to 46 MHz after the hybridization of previous two antennas as shown in Figure 7(c). Antenna III reactance part equals that of ASIC at 922 MHz while resistance matches at 876 MHz. This hybridization lowers the resistance and reactance of tag for lower frequencies. Now, after putting MIL in Antenna II, this tag is again inductive for the same frequency band-range, but it is inductive in the range of 861 MHz to 926 MHz. The resistance matching happens at 855 MHz while the same happens for reactance at 897 MHz. Thus, the matching gap is reduced to 42 MHz. Further, putting MIL in Antenna III, reactance part matches to ASIC at 923 MHz, and the same happens for resistance at 883. Hence, the gap is reduced to 40 MHz. Finally, putting a metal bar on both sides of Antenna V introduces high inductive impedance, and impedance matching happens at 866 MHz with the impedance of $20.62 + j190.94\Omega$ as shown in Figure 7(f).

4. PARAMETRIC SCRUTINY

Different outcomes on reflection coefficient and impedance are produced by every single parameter of proposed antenna. Parametric scrutiny is done by changing single parameter at a time and keeping others constant to check those effects. The impact of alteration of meander line height (h) and meandered-inductive loop separation from feed line (d) on input impedance and reflection coefficient is investigated. The variation of h elaborates the effect of meander line, and the variation of d indicates the effect of MIL separation from feeding line on impedance matching.

To evaluate the response of height of the meander line and return loss on input impedance, tag is simulated by altering parameter h from 10.4 mm to 11.2 mm while retaining others constant. It is comprehended from Figure 8(a) that both real and imaginary parts match with respective values of semiconductor-chip at lower frequency as h increases. Also, we can see the impedance value increases as h increases at 866 MHz. When h is 10.4 mm, we see the real part of impedance matches on 866 MHz with the semiconductor-chip reactance while the same happens for imaginary part on 874 MHz. Hence, matching difference is found to be 8 MHz, and tag antenna resonates at 874 MHz with poor reflection coefficient.

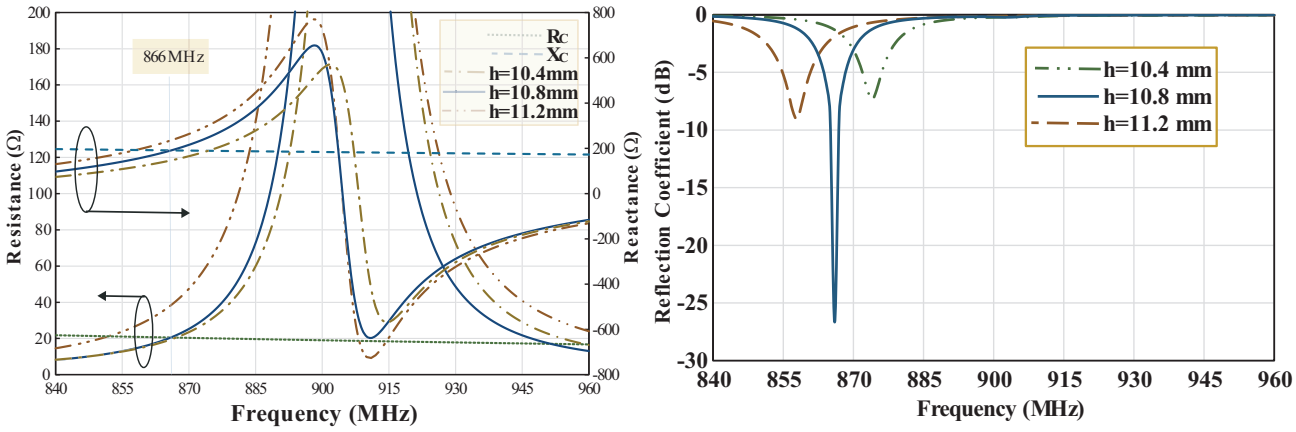

Figure 8. (a) Simulated input impedance and (b) Reflection Coefficient after variation of h.

For $h = 10.8$ mm, it is perceived that the antenna resonates at 866 MHz. When $h = 11.2$ mm, we see the real part of impedance matches on 851 MHz with microchip resistance at 851 MHz while the same happens for imaginary part at 858 MHz. For this value, matching difference is found to be 7 MHz, and tag antenna resonates at 858 MHz with poor reflection coefficient. The reflection coefficient for

above values of h is displayed in Figure 8(b). Thus, the optimum value of h is found to be 10.8 mm.

For investigating the impact of d on performance of this RFID antenna, it is altered from 0.4 mm to 1.2 mm while others are retained constant.

It is comprehended from Figure 9(a) that both real and imaginary parts match with respective values of semiconductor-chip at higher frequency as d increases. We can also see that the impedance value decreases as d increases at 866 MHz. When d is 0.4 mm, impedance matching for real part happens at 859 MHz while that of imaginary part happens at 863 MHz. Thus, we find the difference between them is 4 MHz, and tag antenna resonates at 874 MHz with poor reflection coefficient. When $d = 1.2$ mm, the matching of real part of tag antenna happens at 865 MHz while that of reactance happens at 867 MHz. At this value, the difference is 2 MHz, and antenna resonates at 867 MHz with poor reflection coefficient. The reflection coefficients for above values of d are displayed in Figure 9(b). Thus, from Figure 9, it is noticed that optimum reflection coefficient is achieved for $d = 0.8$ mm.

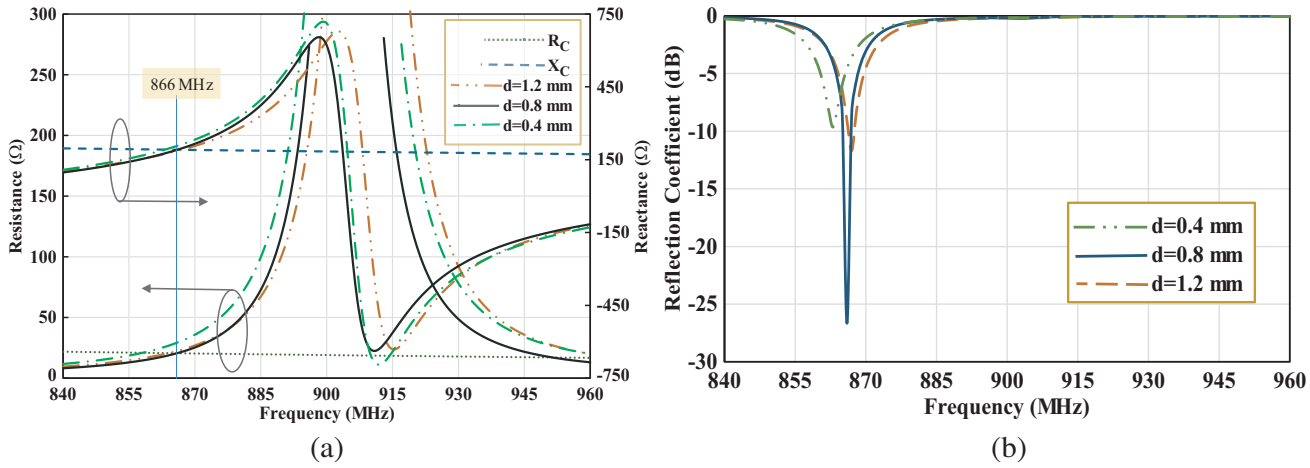

Figure 9. (a) Simulated input impedance and (b) Reflection Coefficient after variation of d.

5. RESULTS AND DISCUSSION

The prototype of fabricated meandered inductive-coupled loop RFID tag antenna with an FR4 substrate is shown in Figure 10. The measurement setup with Vector Network Analyzer is displayed in Figure 11. The scattering-parameters of this proposed antenna were measured by Anritsu (MS2038C) VNA, and

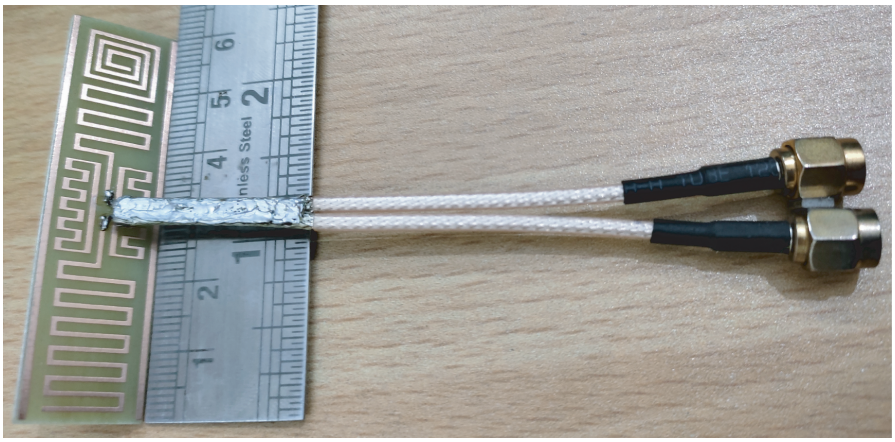

Figure 10. Fabricated proposed RFID tag antenna with differential-probe.

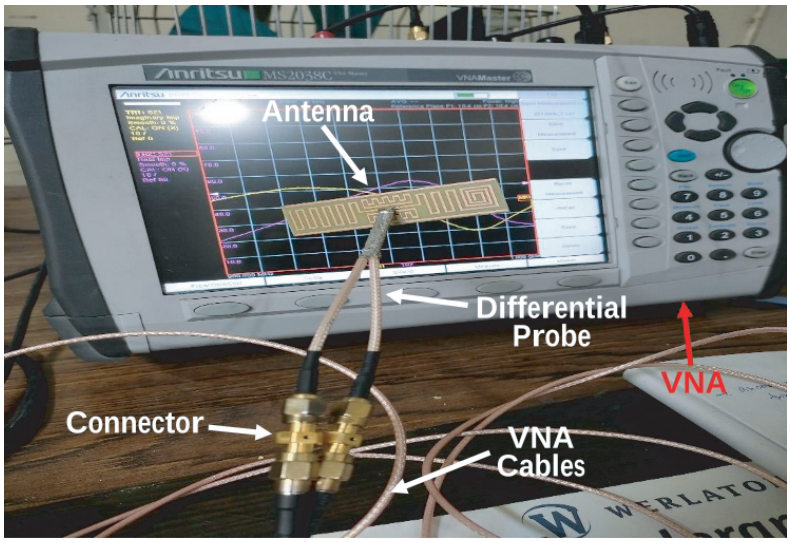

Figure 11. Measurement of UHF Tag.

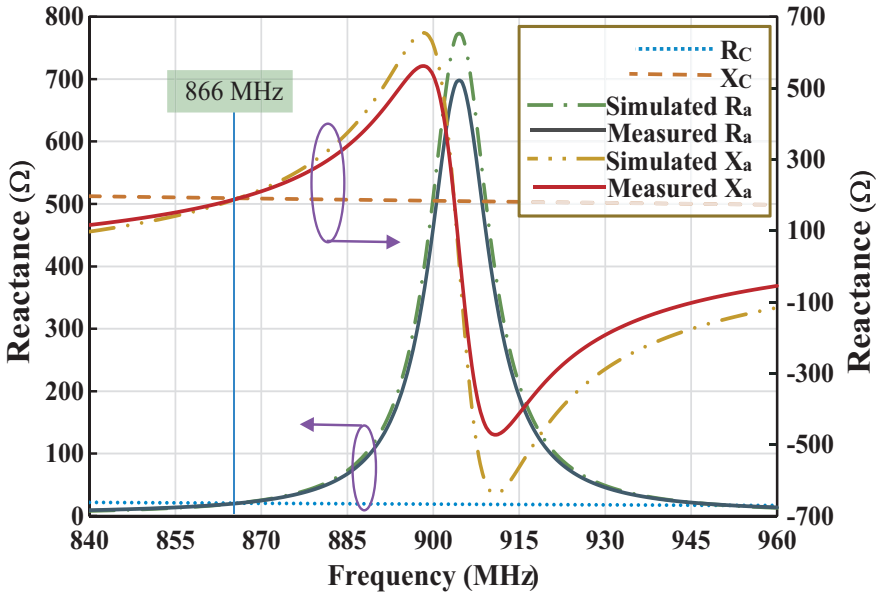

Figure 12. Measured amd simulated input impedance of tag antenna.

then by using subsequent formula, the differential input impedance (Z_{diff}) of tag antenna is calculated.

$$Z_{diff} = 2Z_0 \frac{(1 + S_{12}S_{21} - S_{11}S_{22} - S_{12} - S_{21})}{(1 - S_{11})(1 - S_{22}) - S_{21}S_{12}} \tag{10}$$

The simulated and measured impedances and reflection coefficients of UHF tag are displayed in Figures 12 and 13, respectively. The measured input impedance is $20.6 + j190.9\Omega$ at 866 MHz, which is almost complex conjugate to semiconductor-chip impedance.

Figure 14 shows the radiation pattern of proposed antenna at 866 MHz. It can be seen that this antenna produces a good radiation performance, attains quasi-isotropic radiation pattern, and looks analogous to that of dipole.

The maximum possible separation between reader and tag for switching-on semiconductor-chip,

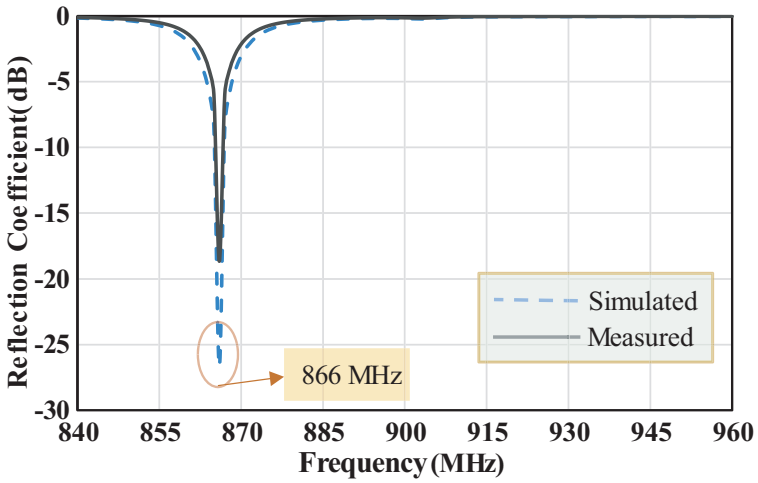

Figure 13. Measured and simulated reflection coefficient of RFID tag.

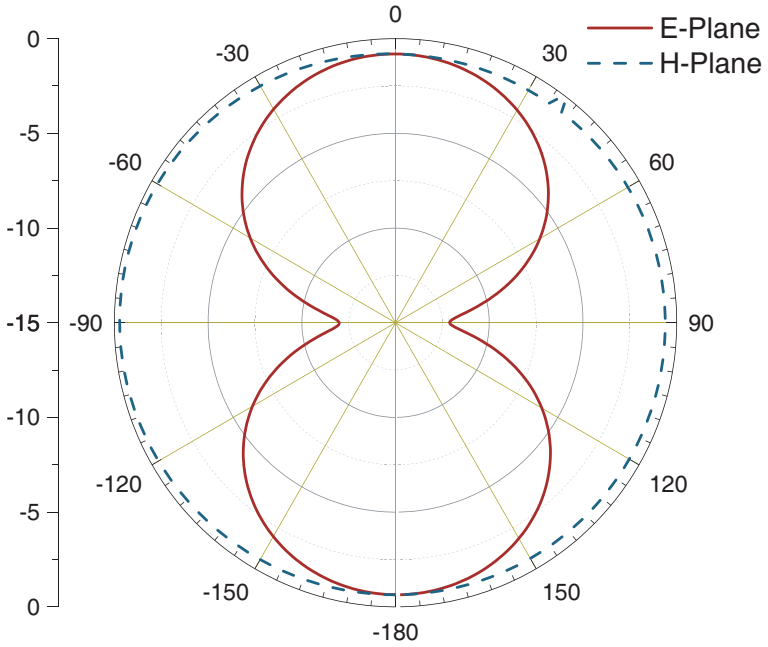

Figure 14. Far-field radiation pattern for E-plane and H-plane at 866 MHz.

i.e., read range, is given by the formula given in Eq. (11).

$$S_{\max}(\theta,\phi) = \frac{\lambda}{4\pi}\sqrt{\frac{EIRP_R}{P_{th,chip}}(1-|\Gamma|^2)G_t(\theta,\phi)} \tag{11}$$

where $G_t(\theta,\phi)$ represents the gain, Γ the voltage reflection coefficient, and $(1-|\Gamma|^2)$ the power transmission coefficient. The tag is evaluated for 4W EIRP reader.

The $G_t(\theta,\phi)$ is further expressed by,

$$G_t(\theta,\phi) = (1-|\Gamma|^2)\eta_{cd}D \tag{12}$$

where η_{cd} is the radiation efficiency, and D is the directivity.

The maximum separation between tag and reader, obtained from Eq. (11), is plotted in Figure 15. The tag read range attains its maximum value up to 12.6 meters at 866 MHz. At airports, luggage

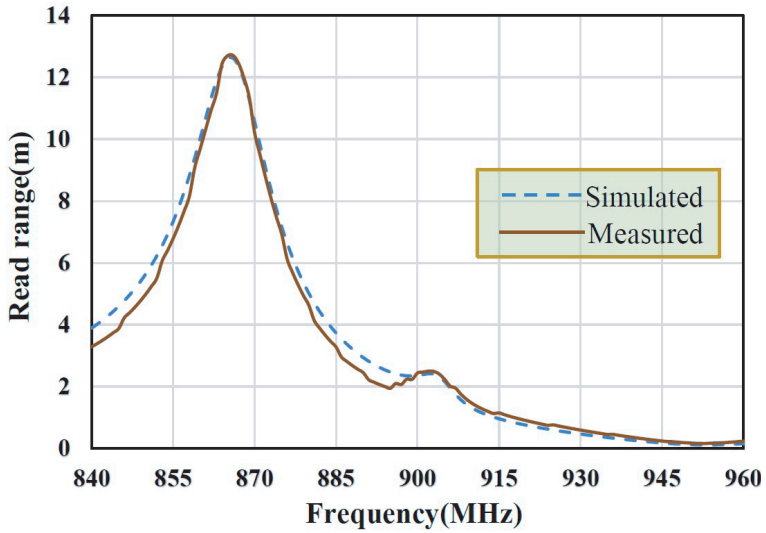

Figure 15. Maximum separation between reader and tag.

orientation can change, so a circularly polarised antenna is installed in RFID reader. Since the proposed tag antenna is linearly polarised in nature, and radiation pattern is bidirectional with significant read range, this tag antenna is applicable at airports for luggage tracking irrespective of reader orientation.

Table 3 analyzes an analogy between this work and other preceding communicated antennas w.r.t. identical operational band in terms of dimensions, used antenna substrate, chip sensitivity, reduction in size and reading territory. This correlation is done for particular UHF tags which were operated in the same proximity of frequency of operation, and also antenna materials used are the same as that of the proposed antenna except [13] and [16]. Although this tag antenna has lower read range than [16], it has 86.67% size reduction. The size reduction percentage shown in Table 3 is for the proposed tag antenna relative to corresponding referenced antenna. It can be seen that by using a meandered dipole, admirable size reduction is achieved. In spite of being tiny tag antenna, this tag antenna provides higher tag-reader separation distance.

Table 3. Distinct parameters correlation of the tendered antenna with few preceding communicated antennas.

Antenna	**Dimensions (mm^3)**	**Antenna substrate**	**Chip Sensitivity (dBm)**	**Frequency (MHz)**	**% Size reduction**	**Read range (m)**
[10]	$67 \times 16 \times 1.54$	FR4	-20.5	866	6.96	10.2
[11]	$66 \times 20 \times 1.6$	FR4	-17.4	867 & 956	27.27	5
[12]	$60 \times 20 \times 1.6$	FR4	-20	866 & 912	20	5.5
[13]	$31.5 \times 31.5 \times 3.2$	PP4 foam	-17.8	867	51.6	7.25
[14]	$91 \times 91 \times 1.6$	FR4	-17.4	866 & 952	88.4	3
[15]	$128 \times 50 \times 1.6$	FR4	-16	866 & 915	85	6.8
[16]	$120 \times 60 \times 1.6$	Rogers RT /duroid	-18.5	865	86.67	13.9
Proposed work	$60 \times 16 \times 1.6$	FR4	-18.5	866	-	12.6

6. CONCLUSION

In this article, a novel meandered dipole with spiral end is produced. The antenna impedance is conjugately-matched to Alien Higgs semiconductor-chip of power sensitivity of −18.5 dBm for the maximum power transfer. The equivalent circuit of the tendered antenna is analysed with equations. The proposed RFID tag antenna is operated at 866 MHz. Further, an enhanced reading-territory is obtained. This tag antenna advances its tag to reader length up to 12.6 meters, which makes it applicable to luggage tracking at airports.

REFERENCES

1. Chawla, V. and D. S. Ha, "An overview of passive RFID," *IEEE Communications Magazine*, Vol. 45, No. 9, 11–17, 2007.
2. Ruiz-Garcia, L. and L. Lunadei, "The role of RFID in agriculture: Applications, limitations and challenges," *Computers and Electronics in Agriculture*, Vol. 79, No. 1, 42–50, 2011.
3. Nekoogar, F. and F. Dowla, *Ultra-wideband Radio Frequency Identification Systems*, Springer Science & Business Media, 2011.
4. Yao, Y., Y. Liang, J. Yu, and X. Chen, "Design of a multipolarized RFID reader antenna for UHF near-field applications," *IEEE Transactions on Antennas and Propagation*, Vol. 65, No. 7, 3344–3351, 2017.
5. Rahman, M. M. and A. K. Sarkar, "A method for calculating the resonant frequency of meander line dipole antenna by using antenna's geometrical parameters," *2017 6th International Conference on Informatics, Electronics and Vision & 2017 7th International Symposium in Computational Medical and Health Technology (ICIEV-ISCMHT)*, IEEE, 2017.
6. Tsai, M.-C., C.-W. Chiu, H.-C. Wang, and T.-F. Wu, "Inductively coupled loop antenna design for UHF RFID on-body applications," *Progress In Electromagnetics Research*, Vol. 143, 315–330, 2013.
7. Son, H. W. and C. S. Pyo, "Design of RFID tag antennas using an inductively coupled feed," *Electronics Letters*, Vol. 41, No. 18, 1, 2005.
8. Liao, S. Y., *Microwave Devices and Circuits*, Pearson Education India, 1990.
9. Grover, F. W., *Inductance Calculations: Working Formulas and Tables*, Courier Corporation, 2004.
10. Kumar, M., A. Sharma, and I. J. Garcia Zuazola, "All-in-One UHF RFID tag antenna for retail garments using nonuniform meandered lines," *Progress In Electromagnetics Research Letters*, Vol. 94, 133–139, 2020.
11. Barman, B., S. Bhaskar, and A. K. Singh, "Spiral resonator loaded S-shaped folded dipole dual band UHF RFID tag antenna," *Microwave and Optical Technology Letters*, Vol. 61, 3, 720–726, 2019.
12. Bansal, A., S. Sharma, and R. Khanna, "Compact meandered folded-dipole RFID tag antenna for dual band operation in UHF range," *Wireless Personal Communications*, Vol. 114, No. 4, 3321–3336, 2020.
13. Ooi, S.-Y., P.-S. Chee, E.-H. Lim, Y.-H. Lee, and F.-L. Bong, "Stacked planar inverted-L antenna with enhanced capacitance for compact tag design," *IEEE Transactions on Antennas and Propagation*, Vol. 70, No. 3, 1816-1823, 2021.
14. Barman, B., S. Bhaskar, and A. K. Singh, "Dual-band UHF RFID tag antenna using two eccentric circular rings," *Progress In Electromagnetics Research M*, Vol. 71, 127–136, 2018.
15. Bhaskar, S. and A. K. Singh, "A dual band dual antenna with read range enhancement for UHF RFID tags," *International Journal of RF and Microwave Computer-Aided Engineering*, Vol. 29, No. 7, e21717, 2019.
16. Singh, A. K., S. Bhaskar, and A. K. Singh, "A nested slot and T-match network based hybrid antenna for UHF RFID tag applications," *Progress In Electromagnetics Research C*, Vol. 125, 93–104, 2022.